Journal Pre-proofs

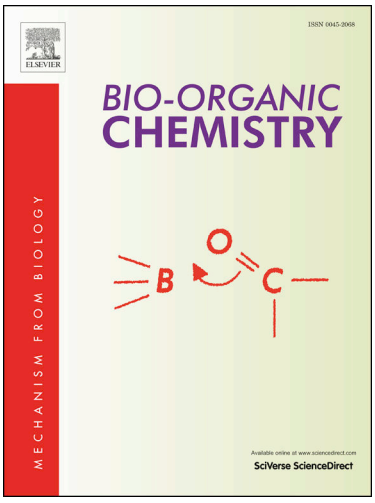

Rare benzonaphthoxanthenones from Chinese folk herbal medicine *Polytrichum commune* and their anti-neuroinflammatory activities in *vitro*

Zi-feng Guo, Guang-ming Bi, Yun-hong Zhang, Jia-heng Li, Da-li Meng

PII: S0045-2068(20)31384-5
DOI: https://doi.org/10.1016/j.bioorg.2020.104087
Reference: YBIOO 104087

To appear in: *Bioorganic Chemistry*

Received Date: 18 March 2020
Revised Date: 15 June 2020
Accepted Date: 7 July 2020

Please cite this article as: Z-f. Guo, G-m. Bi, Y-h. Zhang, J-h. Li, D-l. Meng, Rare benzonaphthoxanthenones from Chinese folk herbal medicine *Polytrichum commune* and their anti-neuroinflammatory activities in *vitro*, *Bioorganic Chemistry* (2020), doi: https://doi.org/10.1016/j.bioorg.2020.104087

Rare benzonaphthoxanthenones from Chinese folk herbal medicine *Polytrichum commune* and their anti-neuroinflammatory activities in *vitro*

Zi-feng Guo[a], Guang-ming Bi[a], Yun-hong Zhang[a], Jia-heng Li[a] and Da-li Meng[a, *]

[a] School of Traditional Chinese Materia Medica, Shenyang Pharmaceutical University, Shenyang 110016, PR China

Corresponding Authors:

*E-mail: mengdl@163.com

Abstract: Two new (**1**-**2**) as well as five known (**3**-**7**) compounds were isolated from *Polytrichum commune*, a folk herbal medicine in China, and three of them (**2**, **4**, **5**) belong to benzonaphthoxanthenones that are rarely found in nature. Their structures were elucidated by the approach to 1D and 2D NMR spectra. The absolute configuration of **2** was assigned by comparing its experimental and calculated ECD data. **1**-**5** were investigated for their anti-neuroinflammatory activity against LPS-induced BV-2 cells. **1** and **3** exhibited well protective effect at a concentration of 2.5 μmol/mL. Molecular docking studies were adopted to further investigate the possible mechanism, whose results suggested that **1** might exert anti-neuroinflammatory effect by inhibiting activity of p38α, JNK2 and TAK1 to reduce the liberation of pro-inflammatory cytokines.

Keyword: *Polytrichum commune*, Chemical Component, Benzonaphthoxanthenones, Anti-inflammatory Effect, Molecular Docking.

1. Introduction

Alzheimer's disease (AD), a global health issue, is the most common type of dementia, accounting for more than two-thirds of all cases. Indeed, 50 million individuals have suffered from dementias worldwide and the number will increase to approximately 152 million by 2050 [1]. As a devastating neurodegenerative disease, AD is mainly characterized by extracellular amyloid-β (Aβ) deposits and intracellular neurofibrillary tangles composed of phosphorylated tau (p-tau), leading to the progressive loss of mental and physical capacities, as well as the functional decline in learning ability [2,3]. Meanwhile, the latest genomics, bioinformatics, functional and epidemiological studies indicate that the microglia-dominated neuroinflammatory process is closely linked with multiple AD pathways [4]. In general, activated microglia cells play a vital role in removing damaged neurons and infectious agents. However, long-term and sustained activation could result in excessive production of proinflammatory cytokines in cerebrospinal fluid, such as interleukin (IL-1β and IL-6) and tumor necrosis factor (TNF-α) [5]. These mediators might directly induce neuronal apoptosis or amplify the local inflammatory response, which caused possible synaptic dysfunction or neuronal loss [6]. Therefore, suppressing the overactivation of microglia is considered as a potential therapeutic strategy for AD.

Polytrichum commune, belonging to the family of *Polytrichum*, is distributed mainly in plain and hilly areas in China, America, Europe, Oceania and Africa. As a Chinese herbal medicine in folk, the dried whole plant of *P. commune* is widely used to treat memory decline and other related diseases in Tujia Minority of China. Potential active compounds have been isolated from *P. commune*, including benzonaphthoxanthenones, cinnamoyl bibenzyls and coumarins [7,8]. Ohioensin F shows anti-inflammatory activity, indicating that benzonaphthoxanthenones may also have potential anti-inflammatory activity [9]. Meanwhile, it is suggested that *P. commune* acts on memory decline and other related diseases through its anti-inflammatory activity possibly. In order to study active compounds and mechanism of action of *P. commune*, a variety of research work was carried out.

In this study, two new (**1**-**2**) and five known (**3**-**7**) compounds were isolated from *P. commune* (**Figure.1**) and three of these seven compounds were benzonaphthoxanthenones. Compounds (**1**-**5**) were evaluated for their anti-inflammatory effects and the potential mechanisms of anti-neuroinflammation were discussed with the method of molecular docking.

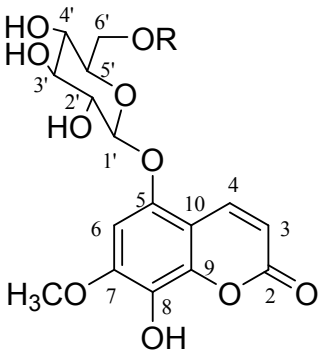

1 R=CH_3CO
3 R=H

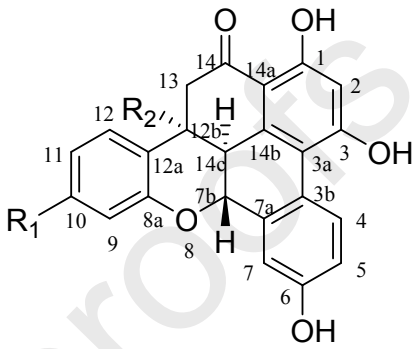

2 R_1=OH R_2=H
4 R_1=H R_2=H
5 R_1=H R_2=OH

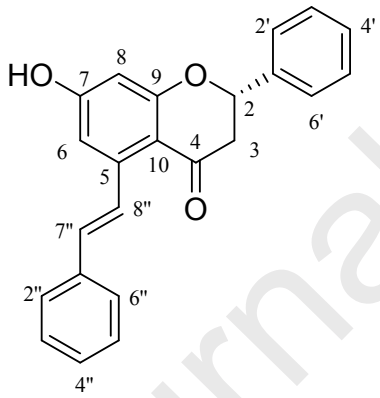

6

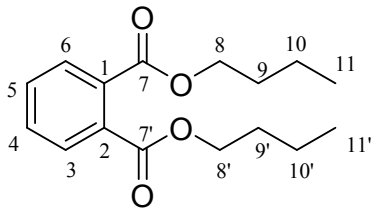

7

Figure.1 Chemical components isolated from *P. commune*

2. Results and Discussion

2.1 Phytochemistry

Compound **1** was isolated as a white powder. The molecular formula $C_{18}H_{20}O_{11}$ was determined based on HRESIMS (*m/z* 435.0905 $[M+Na]^+$ (calcd for 435.0903)) and NMR data, indicating 9 degrees of unsaturation. **1** displayed signals of a coumarin moiety [δ_H 6.22 (1H, d, *J*=9.6 Hz), 8.20 (1H, d, *J*=9.6 Hz). δ_C 160.2, 111.5, 139.9, 146.4, 97.6, 151.5, 128.9, 143.0, 104.9], and a glucose unit [δ_H 4.91 (1H, d, *J*=7.02Hz); δ_C 102.2, 73.5, 76.3, 70.3, 74.3, 64.2], respectively. Meanwhile, one methoxy signals at

δ_H 3.89 (3H, s) and δ_C 56.7, one phenolic hydroxyl signal at δ_H 9.05 (1H, s), one methyl signals at δ_H 1.97 (3H, s) and δ_C 21.0, and one typical carbonyl at δ_C 170.5 were also observed in the 1D NMR spectrum. Exhaustive analysis on the 1D NMR data (**Table.1**) showed that **1** had a similar structure to that of 5,8-dihydroxy-7-methoxycoumarin-5-*β*-glucopyranoside [10]. However, the extra presence of carbonyl signal (δ_C 170.5) and methyl signals (δ_H 1.97, δ_C 21.0) in **1** instead of the active hydrogen in 1D NMR indicated the acetyl substitution on the glucose group, which could be confirmed by the cross peak from δ_H 1.97 to δ_C 170.5 and the δ_H 2.88 to δ_C 170.5 in HMBC spectrum (**Figure.2**). Meanwhile, the downfield shift of C-6' implied the acetyl was linked to the C-6'. Therefore, the structure of **1** was determined and named as 5,8-dihydroxy-7-methoxycoumarin-5-*β*-(6-O-acetyl) glucopyranoside.

Table.1 ^{1}H-NMR data measured at 600 MHz and ^{13}C-NMR data measured at 150 MHz in DMSO-d_6 for Compounds 1-2.

Position	1		2	
	δ_C	δ_H (*J* in Hz)	δ_C	δ_H (*J* in Hz)
1	-	-	161.5	-
2	160.2	-	102.4	6.35, s
3	111.5	6.22, d (9.6)	164.2	-
3a	-	-	115.1	-
3b	-	-	139.7	-
4	139.9	8.20, d (9.6)	115.3	6.74, dd (8.7, 2.5)
5	146.4	-	121.9	8.31, d (8.6)
6	97.6	6.78, s	156.5	-
7	151.5	-	111.5	7.24, d (1.9)
7a	-	-	114.0	-
7b	-	-	70.0	4.96, d (13.7)
8	128.9	-	-	-
8a	-	-	145.4	-
9	143.0	-	117.9	6.72, d (2.6)
10	104.9	-	151.8	-
11	-	-	115.8	6.65, dd (8.7, 2.7)
12	-	-	129.7	6.86, d (8.7)
12a	-	-	124.9	-
12b	-	-	28.2	3.48, dd (13.7, 5.1)
13	-	-	42.5	2.67, dd (15.1, 4.4 13α-H); 2.95, dd (15.1, 4.4 13β-H)
14	-	-	200.9	-
14a	-	-	110.3	-
14b	-	-	139.8	-
14c	-	-	38.1	3.16, dd (13.8, 7.7)
7-OCH_3	56.7	3.89, s	-	-
Glc				
1'	102.2	4.91, d (7.02)	-	-
2'	73.5	-	-	-
3'	76.3	-	-	-
4'	70.3	-	-	-
5'	74.3	-	-	-

6’	64.2	-	-	-
6’-$COCH_3$				
1‘’	170.5	-	-	-
2‘’	21.0	1.97, s	-	-

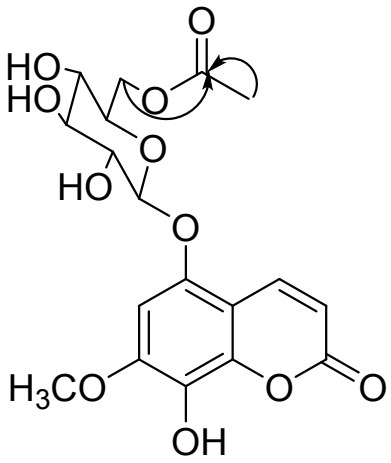

Figure.2 Structure and key HMBC correlations of compound 1

Compound **2** was obtained as a yellow powder in MeOH. Its molecular formula was determined as $C_{23}H_{15}O_6$ based on the HRESIMS at *m/z* 387.0867 $[M+H]^+$ (calcd for 387.0874). **2** had the similar ^{1}H-NMR (600 MHz, DMSO-d_6) and ^{13}C-NMR (150 MHz, DMSO-d_6) data (**Table.1**) to that of ohioensin A [11]. The significant down-filed shifting of carbon resonance of C-10 from δ 128.9 to δ 151.8 indicating hydroxy was attached to the C-10. The key correlations from δ_H 6.86 (1H, d, *J*=8.7, H-12) to δ_C 28.2 (C-12b), δ_H 6.72 (1H, d, *J*=2.6 Hz, H-9), δ_H 6.86 (1H, d, *J*=8.7 Hz, H-12) to δ_C 115.8 (C-11) in HMBC spectrum also confirmed the substitution of hydroxy on C-10 (**Figure.3**). In NOESY spectrum, the cross peak between δ_H 3.48 (1H, dd, *J*=13.7, 5.1 Hz, H-12b) and δ_H 3.16 (1H, dd, *J*=13.8, 7.7 Hz, H-14c) revealed the relative configuration of **2** was 7b*R**, 12a*S**, 14c*S** (**Figure.3**). The absolute configuration of **2** was defined as 7b*R,* 12a*S*, 14c*S* by comparison of the experimental CD with the calculated ECD (**Figure.3**), which was marked as a new compound and named ohioensin I.

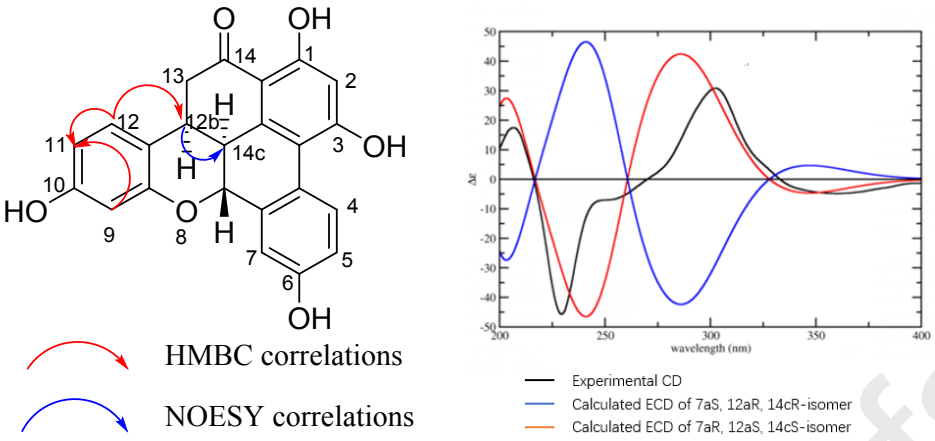

Figure.3 Left: key HMBC and NOESY correlations of compound 2; Right: Comparison of experimental CD with calculated ECD of compound 2

By a combination of spectroscopic and spectrometric methods and comparisons with reported data. The known compounds **3**-**7** were identified as 5,8-dihydroxy-7-methoxycoumarin-5-*β*-glucopyranoside (**3**) [12], ohioensin A (**4**) [11], ohioensin F (**5**) [13], communin B (**6**) [14], dibutyl-phthalate (**7**) [15], respectively.

2.2 Anti-Neuroinflammation Effects Assay

Pathologically, AD mainly includes plaques formed by extracellular A*β* deposits and neurofibrillary tangles composed of p-tau in nerve cells. toxic environment produced by A*β* accumulation induces the sustained stimulation of microglia cells, leading to increasing production of proinflammatory mediators. Meanwhile, an inflammatory environment might activate the tau hyperphosphorylation kinases to promote the formation of neurofibrillary tangles [16]. The loss of tau's normal microtube-stabilizing function would compromise axonal transport and thus lead to the synaptic dysfunction and neurodegeneration. As a consequence, anti-neuroinflammation is considered as a potential therapeutic strategy for AD.

In order to investigate the anti-neuroinflammatory effects of compounds (**1**-**5**), the safe concentrations range of compounds was preliminarily obtained by cytotoxic assay. BV2 microglial cells were treated with compounds (**1**-**5**) and aglycon of compound **1** and **3** at different concentrations (12.5, 25, 50, 100 and 200 *μ*mol/mL). The cell viability of BV2 microglia cells was measured with CCK-8 assay. As shown in **Figure.4**, when the concentrations of compounds were lower than 25 *μ*mol/mL, the cell viability of BV2 microglial were over 75%.

According to the result of cytotoxic assay, LPS-induced BV2 microglial cells were treated with compounds **(1-5)** and aglycon at the concentrations of 1.25, 2.5, 5, 10 and 20 μmol/mL, respectively and CCK-8 assay was used for measuring their cell viability. The results demonstrated that **1** and **3** at 2.5 μmol/mL exhibited more potent anti-neuroinflammatory effects than that of positive control, curcumin, with the significantly increased cell viabilities of 98.99% (P<0.001) and 95.38% (P<0.05), respectively (**Figure. 5**). On the contrary, the aglycon of **1** and **3** and other three compounds didn't show satisfied activities (**Table.2**).

It is widely acknowledged that TNF-α, IL-6 and IL-1β are the major proinflammatory cytokines produced by LPS-induced BV2 cells [17]. To further study the anti-neuroinflammatory mechanism, the effects of these compounds on the regulation of TNF-α, IL-6, IL-1β in LPS-stimulated BV2 microglia cells were analyzed by ELISA. According to the results of cell viability assay, 2.5 μmol/mL was used as the test concentration for these six compounds. As shown in **Figure.6**, LPS significantly increased the production of inflammatory mediators in BV2 microglia cells including IL-1β, IL-6 and TNF-α (P<0.01, 0.001, and 0.01, respectively). However, compound **1** markedly inhibited release of these crucial inflammatory cytokines (P<0.001, 0.01, and 0.05, respectively), which was almost better than the positive control, suggesting that **1** was the most possible anti-neuroinflammatory constituent in this plant.

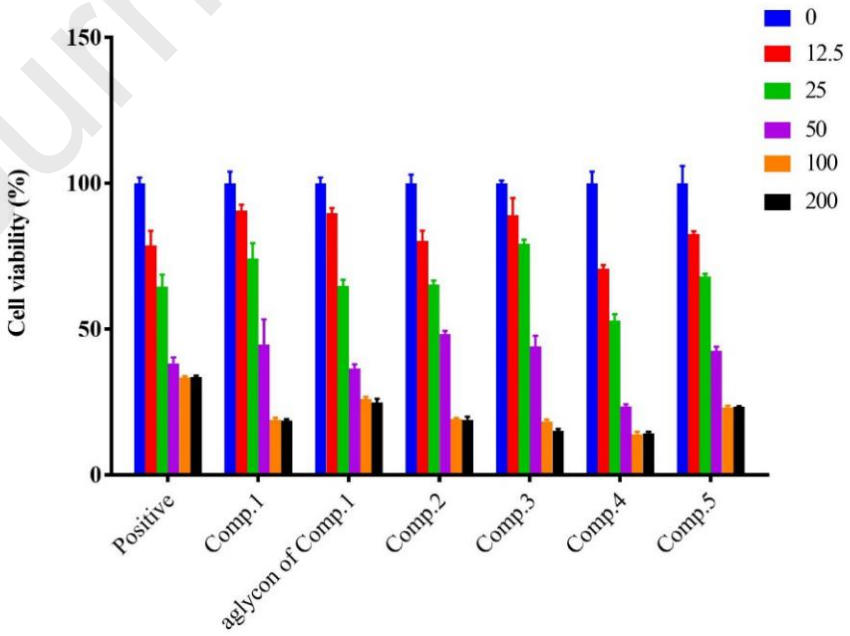

Figure.4 treated with comp.1-5, aglycon of compound 1 and curcumin at different concentrations (12.5, 25, 50, 100 and 200 μmol/mL). Cell viability was measured with a CCK-8 assay. The data are expressed as the percentage of the relative untreated control cells. All values are expressed as the mean ± SD of three independent experiments.

Table.2 Anti-neuroinflammatory effects against LPS-induced BV2 microglia cells

Concentration (μmol/mL)	Cell viability						
	positive	Comp 1	aglycon of 1	Comp 2	Comp 3	Comp 4	Comp 5
1.25	99.89%±0.03	99.38%±0.01	90.23%±0.09	94.35%±0.02	97.95%±0.03	90.08%±0.03	88.99%±0.03
2.5	98.29%±0.02	98.99%±0.03	80.24%±0.06	80.86%±0.01	95.38%±0.05	86.85%±0.05	83.54%±0.01
5	90.86%±0.02	88.45%±0.01	76.25%±0.05	73.54%±0.06	87.64%±0.02	79.75%±0.06	80.54%±0.04
10	85.57%±0.06	87.85%±0.02	75.38%±0.01	60.58%±0.04	79.95%±0.03	76.945%±0.03	79.03%±0.06
20	84.61%±0.09	88.03%±0.02	74.99%±0.02	61.23%±0.02	80.63%±0.08	74.22%±0.01	78.56%±0.01

Each value represents the mean ± SD of three independent experiments.

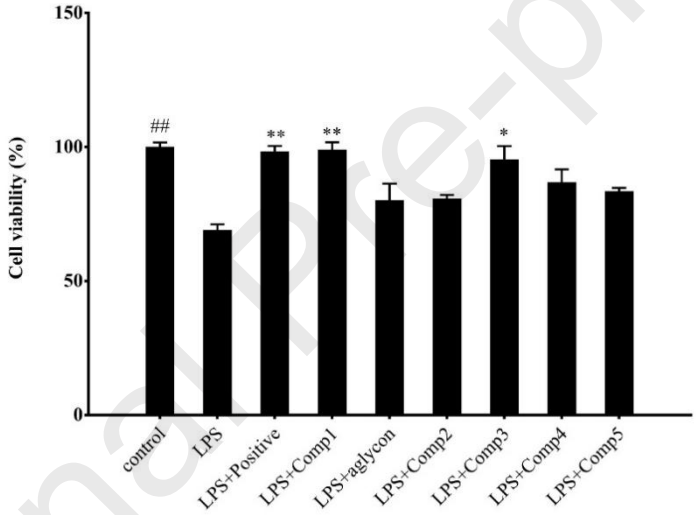

Figure.5 Treated with comp. 1-5, aglycon of 1 and curcumin at 2.5 μmol/mL. Cell viability was measured with a CCK-8 assay. The data are expressed as the percentage of the relative untreated control cells. All values are expressed as the mean ± SD of three independent experiments. *P<0.05, **P<0.01, ***P<0.001 vs the LPS-induced group, $^{\#}P$<0.05, $^{\#\#}P$<0.01, $^{\#\#\#}P$<0.001 vs LPS-induced group.

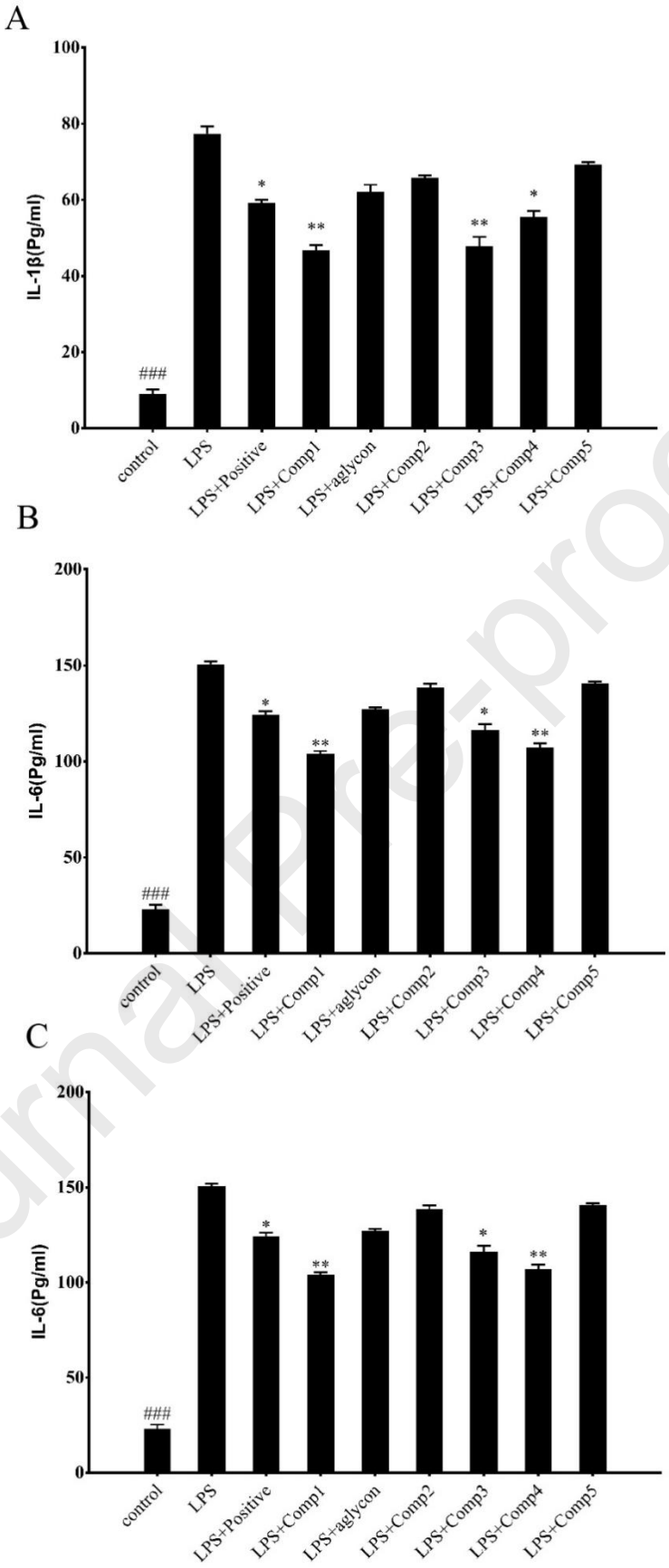

Figure.6 Effects of comp.1-5 on LPS-induced IL-1β, IL-6 and TNF-α production in BV-2 microglial cells. Levels of IL-1β (7A), IL-6 (7B) and TNF-α (7C) in the supernatants were

determined by ELISA. All values are expressed as the mean ± SD of three independent experiments. *P<0.05, **P<0.01, ***P<0.001 versus the LPS-induced group, $^{\#}P$<0.05, $^{\#\#}P$<0.01, $^{\#\#\#}P$<0.001 vs LPS-induced group.

2.3 Molecular Docking

Docking studies were carried out using Molegro Virtual Docker in the active sites of five hub targets of inflammation in order to investigate the possible interactions between the compounds **1-5** and the active site of the targets, namely, ERK1 (PDB ID: 6GES), p38α (PDB ID: 6QDZ), JNK2 (PDB ID: 3E7O), IKKβ (PDB ID: 4KIK) and TAK1 (PDB ID: 5V5N). The docking scores were depicted in **Table.3**, in which compound **1** showed the best effect on all five proteins due to its lower scores among all compounds. Based on the docking scores and the results of anti-neuroinflammatory effects assay *in vitro*, further docking study of compound **1** was carried out.

Table.3 Results of molecular docking studies of comp. 1-5 in the active sites of proteins (PDB code 6GES, 6QDZ, 3E7O, 4KIK and 5V5N) performed using Molegro Virtual Docker.

Compound	ERK1	p38α	JNK2	IKKβ	TAK1
curcumin	-113.123	-139.866	-138.275	-107.128	-132.033
1	-94.8697	-138.532	-115.827	-81.5805	-109.596
aglycon	-71.6578	-89.0226	-74.1528	-58.9881	-63.611
2	-76.7099	-110.091	-117.014	-79.8196	-108.861
3	-83.9532	-120.837	-94.0528	-81.4911	-94.7044
4	-74.5631	-113.145	-110.04	-70.782	-100.36
5	-73.957	-106.864	-106.782	-65.478	-98.4667

Before docking, the X-ray structure of localization inhibitors in ERK1 (N-{2-[(5-chloro-2-{[4-(4-methylpiperazin-1-yl)phenyl]amino}pyrimidin-4-yl)amino]phenyl}propanamide), p38α (2-fluoro-4-[4-(4-fluorophenyl)-1H-pyrazol-3-yl]pyridine), JNK2 (N-{3-[5-(1H-1,2,4-triazol-3-yl)-1H-indazol-3-yl]phenyl}furan-2-carboxamide), IKKβ (K-252A) and TAK1 (N~1~-(1-propyl-1,3-dihydro-2H-benzimidazol-2-ylidene)benzene-1,3-dicarboxamide) were taken from the PDB. The root mean square deviations (RMSDs) of proteins crystalized with localization inhibitors were 2.07 Å, 1.73 Å, 2.14 Å, 2.83 Å, 2.006 Å and 2 Å, respectively, which demonstrated that the docking procedure could be relied to predict the binding mode of our compounds.

The binding mode of compound **1** in the active site of p38α is represented in its 3D mode and schematic 2D in **Figure.7**, showing the H-bond interactions formed by the hydroxyl from glycosyl with GLU 192 and LEU 291. The other key residues which

involved in interaction were ILE 250, TRP 197and LYS 249. This score (-138.532) was found to be approach the docking score (-139.866) of the reference ligand.

The binding mode of compound **1** in the active site of JNK2 is represented in its 3D mode and schematic 2D in **Figure.7**, which showed three H-bond interactions including the ester group from glycosyl with MET 111 and the hydrogen from glycosyl with ILE 32, GLN 117. The other key residues which involved in interaction were LEU 168 and VAL 40.

The binding mode of compound **1** in the active site of TAK1 is represented in its three-dimensional mode and schematic 2D in **Figure.7**. Four H-bond interactions were obsrved, including the carbonyl group from coumarin skeleton with LYS 63, the hydrogen from coumarin skeleton with GLU 105 as well as the hydrogen from glycosyl with PRO 160 and ARG 44. The other key residues which involved in interaction were LEU163, ALA 61, VAL 50, MET 104, CYS 174, ALA 107 and VAL 42.

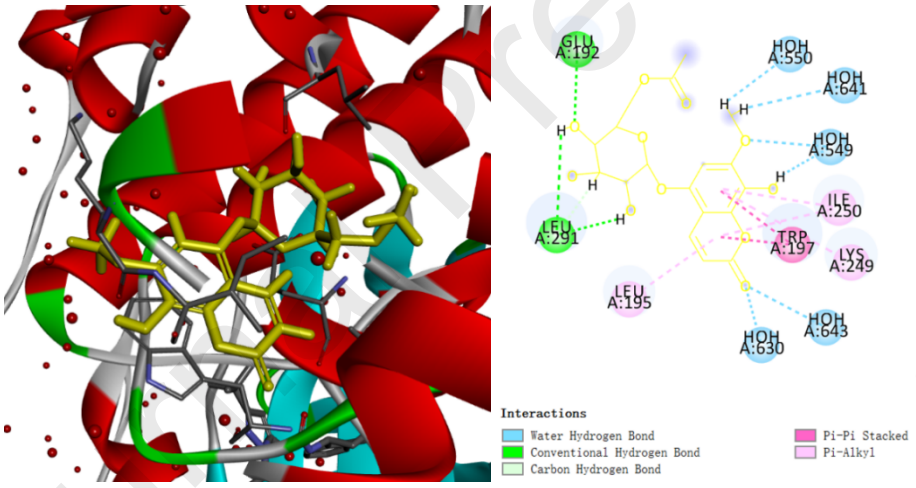

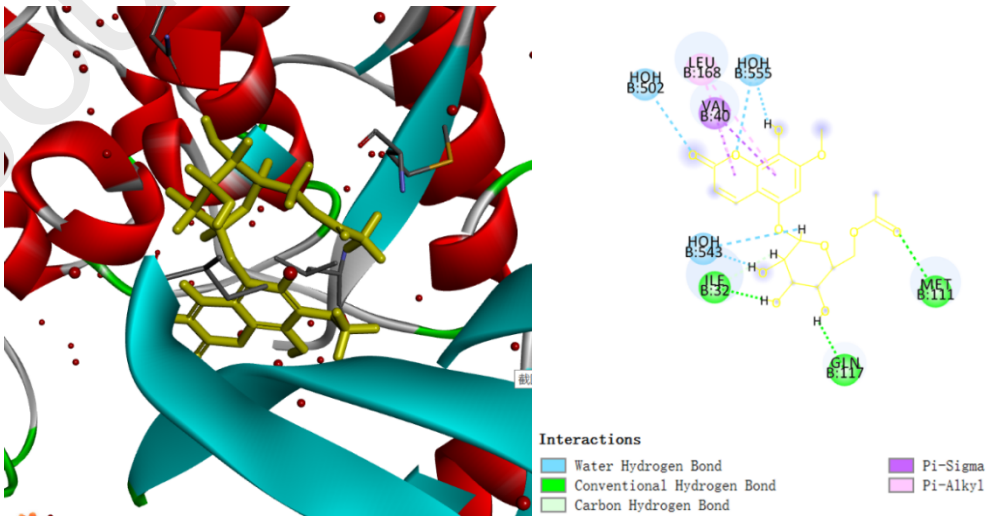

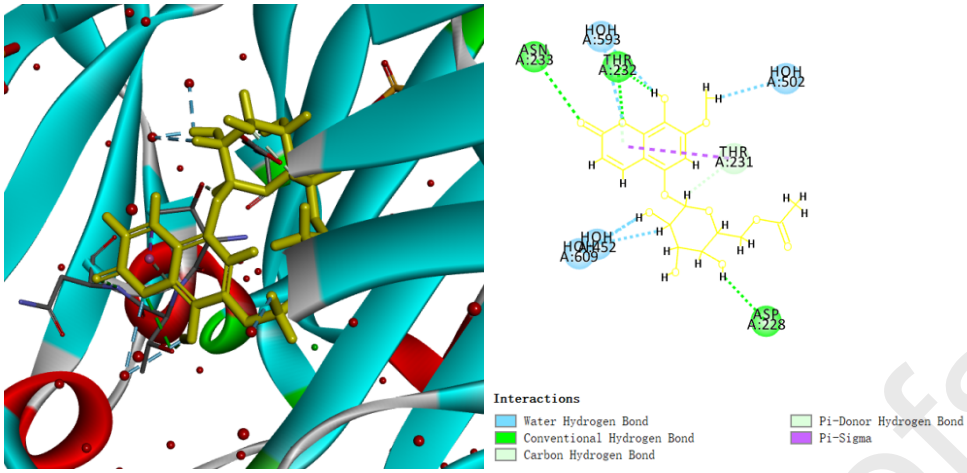

Figure.7 Schematic (2D) representation and Schematic (3D) representation that molecular model of the compound 1 was in the proteins p38α, JNK2 and TAK1. Top: protein p38α (protein data bank ID chimeric 6QDZ). Middle: protein JNK2 (protein data bank ID chimeric 3E7O). Bottom: protein TAK1 (protein data bank ID chimeric 5V5N).

In TAK1-NF-*κ*B signaling pathway, NF-*κ*B plays the important role in inflammation process as a transcription factor. In resting cells, transcriptional activity of NF-*κ*B is blocked *via* binding with inhibitory kappa B (I*κ*B) proteins. Upon activation, inhibitor of *κ*B kinase (IKK) is activated by TGFβ-activated kinase (TAK1) *via* phosphorylating two serine residues in the activation site. IKK guide the degradation of I*κ*B *via* phosphorylation, thereby, releasing NF-*κ*B [18,19]. In addition to NF-KB pathway, MAPK signaling pathway also play a critical role in neuroinflammation. *In vivo* studies suggest that ERK, p38 and JNK are considered as very important regulators of inflammatory mediators [20.21]. Therefore, the results of molecular docking revealed that the anti-neuroinflammatory activity exhibited by compound **1**, whose docking scores with proteins TAK1, p38α and JNK2 were high, might be a result of activating the TAK1-NF-*κ*B and MAPK pathways.

In conclusion, compound **1** could effectively reduce the production of pro-inflammatory mediators, including TNF-α, IL-6 and IL-1β. Meanwhile, molecular docking studies suggested that **1** showed strong interaction with the proteins p38α, JNK2 and TAK1, indicating that 1 was promising to be explored as a neuroprotective drug. Therefore, further studies of anti-neuroinflammation effects and corresponding mechanisms are still needed.

3. Experimental section

3.1 General Experimental Procedures

Optical rotations were measured on a JH-P600 automatic multispectral polarimeter. ECD spectra was determined on a Bio-Logic Science MOS-450 spectrometer (Bio-Logic Science Instruments, Seyssinet-Pariset, France). HRESIMS data were obtained using an Agilent 6200 series TOF. Standard pulse sequences were used for all NMR experiments, which were run on Bruker ARX-300 and AV-600 spectrometer, with TMS as an internal standard in dimethyl sulfoxide-d_6 (DMSO-d_6). Column chromatography was run using silica gel (SiO_2 200-300 mesh, Qingdao Haiyang Chemical Group Corporation, Qingdao, China), Sephadex LH-20 (25-100 μm, Green Herbs Science and Technology Development Co., Ltd. China), and reversed-phase C_{18} Silica gel (YMC Co. Ltd., Kyoto, Japan). HPLC separation was done on SHIMADZU HPLC components comprising a SHIMADZU LC-20AR pump and a SHIMADZU SPD-20A ultraviolet detector, with YMC-Pack ODS-A semi-preparative column (250 × 10 mml D, S-5 μm, 12 nm).

3.2 Plant Material

The dried whole plant *P. commune* were collected from Yunnan Province, China on March 2016 and authenticated by prof. Jincai Lu, Shenyang Pharmaceutical University. A voucher specimen (No. 20160815) was deposited in School of Traditional Chinese Material Medica, Shenyang Pharmaceutical University.

3.3 Extraction and Isolation

The dried whole plant of *P. commune* (6 kg) was extracted with 70% ethanol under reflux for 4 h, 3 times. The concentrated crude extract (479.3 g) was then extracted successively with different solvents to obtain petroleum ether (11.5 g), CH_2Cl_2 (25.7 g), and n-BuOH extract (140.1 g), respectively. Then, the n-BuOH extract was subjected to separation over a reduced pressure silica gel, eluting with a gradient system of CH_2Cl_2/MeOH (100:0, 10:1, 3:1 and 1:1) to obtain four fractions, Fr.1 (2 g), Fr.2 (18.4 g), Fr.3 (48.5 g) and Fr.4 (17.6 g), respectively. Fr.2 was further fractionated by MPLC over reversed-phase C_{18} silica gel, using MeOH/H_2O (20:80, 40:60, 60:40, and 80:20) as the elution system, to get four fractions, Fr.2.1 (1.2 g), Fr.2.2 (1.5 g), Fr.2.3 (1.7 g), and Fr.2.4 (2 g), respectively. Fr.2.1 was further purified by recrystallization in

MeOH, to give **3** (100 mg). Fr.2.2 was then purified by Sephadex LH-20 column chromatography, eluting with MeOH, and then purified via HPLC (MeOH/H_2O 42:58) to give **1** (11 mg) and **5** (5 mg). Fr.2.3 was further separated by Sephadex LH-20 which eluted with MeOH and then purified via HPLC (MeOH/H_2O 45:55) to afford **2** (7 mg). Fr.2.4 was also subjected to Sephadex LH-20 which eluted with MeOH to get Fr.2.4.1 and Fr.2.4.2. Fr.2.4.1 was chromatographed over a silica gel column, eluting with CH_2Cl_2-MeOH mixtures (10:1, 3:1) to get **6** (10 mg). Fr.2.4.2 was purified via recrystallization to afford **4** (40 mg). Fr.3.1 was subjected to column chromatography on reversed-phase C_{18} with MeOH/H_2O (20:80, 40:60) to get Fr.2.4.1 and Fr.2.4.2. Fr.2.4.2 was fractionated by Sephadex LH-20 which eluted with MeOH and then purified via HPLC (MeOH/H_2O 54:46) to get **7** (1.8 mg).

3.3.1 5,8-dihydroxy-7-methoxycoumarin-5-β-(6-O-acetyl) glucopyranoside (1)

White powder; ^{1}H-NMR (DMSO-d_6, 600 MHz) and ^{13}C-NMR (DMSO-d_6, 150 MHz) data, see **Table.1**; HRESIMS *m/z* 435.0905 $[M+Na]^+$ (calcd for $C_{18}H_{20}O_{11}$, 435.0903).

3.3.2 Ohioensin I (2)

Yellow powder; $[\alpha]_D^{25}$ -30 (c 1mg/ml, MeOH); ^{1}H-NMR (DMSO-d_6, 600 MHz) and ^{13}C-NMR (DMSO-d_6, 150 MHz) data, see **Table.1**; HRESIMS *m/z* 387.0867 $[M+H]^+$ (calcd for $C_{23}H_{15}O_6$, 387.0874).

3.4 ECD Calculation

The absolute configuration of **2** was defined by using time-dependent density functional theory (TDDFT) calculations [22]. The relative configuration of **2** was subjected to random conformational analysis with the MMFF94s force field to obtain energy minimization by CONFLEX [23]. Conformers whose energy was no more 3 kcal/mol higher than the lowest energy were then imported into the Gaussian 09 software and optimized at the B3LYP/6-31G (d) level. The ECD of the conformers were performed by the TDDFT method at the B3LYP/6-31G (d, p) level with the PCM model in methanol solution, and the overall ECD curves were produced by SpecDis 1.71 [24].

3.5 Acid Hydrolysis

Compound 1 (2.0 mg) was dissolved in 1mL of 1N HCl and heated to 80 ℃ for 3h. This reaction mixture was diluted with H_2O and extracted with CH_2Cl_2. The CH_2Cl_2 extract was evaporated in vacuo to yield aglycon [25].

3.6 Cell Culture

BV2 microglial cells were maintained in Dulbecco's modified eagle's medium (DMEM) supplemented with 10% fetal bovine serum (FBS) and penicillin/streptomycin (100 U/mL and 100 μg/mL, respectively) in a humidified atmosphere of 5% CO_2 at 37 °C. Cells were allowed to grow till it reached a confluency of 80%-90% and was washed with phosphate buffered saline (PBS) with regular replacement of culture medium.

3.7 Cytotoxic Assays

To avoid possible effect of reduced viability on cells, the cytotoxic activities were assayed using CCK-8 method (Dalian Meilun Biotechnology Co., Ltd). The cells were plated in 96-well plate at a density of 1×10^5 cells/ml. After attachment, the cells were preincubated with the test compounds in different concentrations (12.5, 25, 50, 100 and 200 μmol/mL) for 16 h. Then 10 μL CCK-8 was added to the cells and incubated for 2 h. Absorbance was measured by a microplate reader at 450 nm.

3.8 Anti-Neuroinflammatory Assays

The cells were seeded into 96-well plates at a density of 1×10^5 cells/ml. After attachment, the cells were preincubated with the test compounds in different concentrations (1.25, 2.5, 5, 10 and 20μmol/mL) for 2 h, and 20 μL of an LPS solution (diluted with medium to a final concentration of 100 μg/mL) was subsequently added. After preincubation, the treated cells were incubated for 24 h for treatment. Then, 10 μL CCK-8 was added to the cells and incubated for 2 h. Absorbance was measured at a wavelength of 450 nm using a microplate reader. Cell viability was measured using CCK-8 assay. The viability of BV2 microglial cells for the control group (with DMSO only) is defined as 100%. Curcumin was tested as a positive control.

3.9 Determination of Proinflammatory Cytokines Release

The levels of IL-1β, IL-6 and TNF-α in the culture supernatant were determined using the commercially available ELISA kits (Dalian Meilun Biotechnology Co., Ltd). The concentrations were calculated from the standard curves.

3.10 Molecular docking

In order to evaluate predicted targets, the crystal structures of candidate targets were downloaded from RCSB Protein Database (http://www.pdb.org/) and embellished by the Sybyl-X (version 2.0, TRIPOS Inc.) software, including removing the ligands, adding hydrogen, removing water, optimizing and patching amino acids. Before molecular docking, ChemBioDraw 3D was used to make three dimensional chemical structural formulas and energy minimizing for all the compounds, and saved in MOL2 format. Besides, a suitable method of evaluating the precision of a docking procedure was needed. The accuracy and consistency of the docking results modeled by Molegro Virtual Docker (MVD) were checked by comparing the best docking poses between the predicted conformation [26].

3.11 Statistical analysis

The data were reported as mean ± SD. The SPSS Statistics 26.0 was employed for statistical analyses. The statistical significance was determined by one-way AVONA. Values were considered significant at the $P \leqslant 0.05$ level.

Associated Content

Supporting Information

The supporting information (1D and 2D NMR, HERESIMS of compounds **1-2**) to this article can be found online.

Author Information

*E-mail: mengdl@163.com；mengdl@syphu.edu.cn (Da-li Meng)

Notes

The authors declare no conflict of interest.

Acknowledgements

This work was supported by the National Natural Science Foundation of China (Grant No. 81573694), and the project is sponsored by "Liaoning BaiQianWan Talents Program".

Reference

1. Alzheimer's Disease International, World Alzheimer Report 2018-The state of the art of dementia research: New frontiers. https://www.alz.co.uk/research/world-report-2018 , 2018 (accessed 29 August 2019)
2. O' Brien, R.J., and Wong, P.C., Amyloid precursor protein processing and Alzheimer's Disease. Annual Review of Neuroscience, 34 (2011) 185-204. DOI: 10.1146/annurev-neuro-061010-113613
3. Shulman, J.M., De Jager, and P.L., Evidence for a common pathway linking neurodegenerative disease, Nature Genetics, 41 (2009) 1261-1262. DOI: 10.1038/ng1209-1261
4. W.Y. Fu, X.J. Wang, Nancy Y.L., Targeting neuroinflammation as a therapeutic strategy for Alzheimer's Disease: Mechanisms, Drug candidates, and new opportunities, ACS Chem. Neurosci., 10 (2019) 872-879. DOI: 10.1021/acschemneuro.8b00402
5. Hensley, K., Neuroinflammation in Alzheimer's Disease: Mechanisms, Pathologic Consequences, and Potential for Therapeutic Manipulation. Journal of Alzheimer's Disease, 21 (2010) 1–14. DOI:10.3233/jad-2010-1414
6. Agostinho, P., Cunha, R. A., and Oliveira, C., Neuroinflammation, Oxidative Stress and the Pathogenesis of Alzheimer's Disease, Curr. Pharm. Des., 16 (2010) 2766– 2778. DOI: 10.2174/138161210793176572
7. X.X. Cheng, Y.P. Xiao, P. Wang, Y.T. Zhou, H. Yan, Q.H. Liu, Anti-tumor and pro-apoptotic activity of ethanolic extract and its various fractions from *Polytrichum commune L.ex Hedw* in L1210 cells, J. Ethnopharmacol. 143 (2012) 49-56. http://dx.doi.org/10.1016/j.jep.2012.05.054
8. W.J. Yuan, X.X. Cheng, P. Wang, Y.L. Jia, Q.H. Liu, W. Tang, X.B. Wang, *Polytrichum commune L.ex Hedw* ethyl acetate extract-triggered perturbations in

intracellular Ca^{+} homeostasis regulates mitochondrial-dependent apoptosis, J. Ethnopharmacol. 172 (2015) 410-420. http://dx.doi.org/10.1016/j.jep.2015.07.002

9. H.E, Byeon, S.H. Um, J.H. Yim, H.K. Lee, S. Pyo, Ohioensin F suppresses TNF-α-induced adhesion molecule expression by inactivation of the MAPK, Akt and NF-κB pathways in vascular smooth muscle cells, Life sciences, 90 (2012) 396-406. DOI: 10.1016/j.lfs.2011.12.017
10. J. Raubuch, H. Geiger, H.D. Zinsmeister, Coumarin Glycosides from the Mosses *Dendroligotrichum dendroides* and *Dawsonia superba*, Z. Naturforsch. 54c (1999) 456-457. DOI: 0939-5075/99/0500-0456 $ 06.00
11. G.Q. Zheng, C.J. Chang, Ohioensin-A: A Novel Benzonaphthoxanthenone from *Polytrichum ohioense*, J. Am. Chem. Soc. 111 (1989) 5500-5501. DOI: 0002-7863/89/1511-5500$01.50/0
12. M. Jung, H.D. Zinsmeister, H. Geiger, New Three- and Tetraoxygenated Coumarin Glucosides from the Mosses *Atrichum undulatum* and *Polytrichum formosum*, Z. Naturforsch. 49c (1994) 697–702. DOI: 10.1515/ZNC-1994-11-1201
13. C. Seo, Y.H. Choi, J.H. Sohn, J.H. Yim, H.K. Lee, H. Oh, Ohioensins F and G: Protein tyrosine phosphatase 1B inhibitory benzonaphthoxanthenones from the Antarctic moss *Polytrichastrum alpinum*, Bioorg. Med. Chem. Lett. 18 (2008) 772-775. DOI: 10.1016/j.bmcl.2007.11.036
14. P. Fu, S. Lin, L. Shan, Constituents of the Moss *Polytrichum commune*, J. Nat. Prod. 72 (2009) 1335-1337. DOI: 10.1021/np800830v
15. X.L. Wu, H. Liang, X.Y. Wu, Y. Huang, J. Chen, C. Liu, The Chemical Constituents of *Acorus tatarinowii*, Journal of NingXia Medical University. 39 (2017) 53-55. DOI: 10.16050/j.cnki.issn1674-6309.2017.01.014
16. Ballatore C., Lee V. M.-Y., and Trojanowski J.Q., Tau-mediated neurodegeneration in Alzheimer's disease and related disorders. Nature Reviews Neuroscience, 8 (2007):663-672. DOI: 10.1038/nrn2194
17. Mcinnes I.B., Buckley C.D., Isaacs J.D., Cytokines in rheumatoid arthritis - shaping the immunological landscape, Nat. Rev. Rheumatol. 12 (2016) 63-68. DOI: 10.1038/nrrheum.2015.171

18. Chen, Z. J., Ubiquitin signalling in the NF-κB pathway, Nature Cell Biology, 7 (2005) 758–765. DOI:10.1038/ncb0805-758

19. Wang, G., Fu, Y., Ma, K., Liu, J. and Liu, X., NOD2 regulates microglial inflammation through the TAK1-NF-κB pathway and autophagy activation in murine pneumococcal meningitis, Brain Research Bulletin, 158 (2020) 20–30. DOI:10.1016/j.brainresbull.2020.02.006

20. Xu, J., Yuan, C., Wang, G. and Luo, J., et al., Urolithins Attenuate LPS-Induced Neuroinflammation in BV2 Microglia via MAPK, Akt, and NF-*κ*B Signaling Pathways. Journal of Agricultural and Food Chemistry, 66 (2018) 571–580. DOI:10.1021/acs.jafc.7b03285

21. Chowdhury, T. T., Salter, D. M., Bader, D. L., and Lee, D. A., Signal transduction pathways involving p38 MAPK, JNK, NFκB and AP-1 influences the response of chondrocytes cultured in agarose constructs to IL-1β and dynamic compression, Inflammation Research, 57 (2008) 306–313. DOI:10.1007/s00011-007-7126-y

22. C.X. Li, D. Ferreira, Y. Ding, Determination of absolute configuration of natural products: theoretical calculation of electronic circular dichroism as a tool, Curr. Org. Chem. 14 (2010) 1678. DOI: 10.2174/138527210792927717

23. B. Jagannadh, S.S. Reddy, R.P. Thangavelu, Conformational preferences of 1,4,7-trithiacyclononane: a molecular mechanics and density functional theory study, J. Mol. Model. 10 (2004) 55-59. DOI: 10.1007/s00894-003-0166-5

24. Y. Wang, Y.W. Sun, Y.M. Wang, Y. Ju, D.L. Meng, virtual screening of active compounds from *Artemisia argyi* and potential targets against gastric ulcer based on Network pharmacology, Bioorg. Chem. 88 (2019) 102924. https://doi.org/10.1016/j.bioorg.2019.102924

25. Won Se Suh, Chung Sub Kim, Lalita Subedi, Sun Yeou Kim, Sang Un Choi, and Kang Ro Lee, Iridoid Glycosides from the Twigs of Sambucus williamsii var. coreana and Their Biological Activities, J. Nat. Prod, 80 (2017) 2502-2508. DOI: 10.1021/acs.jnatprod.7b00410

26. R. Anwar, New tips for structure prediction by comparative modeling, Bioinformation 3 (2014) 253-266. www.bioinformation.net

Declaration of interests

☒ The authors declare that they have no known competing financial interests or personal relationships that could have appeared to influence the work reported in this paper.

☐The authors declare the following financial interests/personal relationships which may be considered as potential competing interests:

Highlights

A series of rare benzonaphthoxanthenone isolated from *Protrichum commune*
Their anti-neuroinflammatory activities were determined by CCK-8 assay
Molecular docking was carried out to explore potential anti-neuroinflammatory mechanism